

Searches for ultra-high energy gamma-ray at the Pierre Auger Observatory and implications on super-heavy dark matter

Olivier Deligny¹, for the Pierre Auger Collaboration²

¹Laboratoire de Physique des 2 Infinis Irène Joliot-Curie (IJCLab)
CNRS/IN2P3, Université Paris-Saclay, Orsay, France

²Full author list: http://www.auger.org/archive/authors_2024_06.html

E-mail: deligny@ijclab.in2p3.fr

Abstract. The first interactions of photon-induced showers are of electromagnetic nature, and the transfer of energy to the hadron/muon channel is reduced with respect to the bulk of hadron-induced showers. This results in a lower number of secondary muons. Additionally, as the development of photon showers is delayed by the typically small multiplicity of electromagnetic interactions, their maximum of shower development is deeper in the atmosphere than for showers initiated by hadrons. These salient features have enabled searches for photon showers at the Pierre Auger Observatory. They have led to stringent upper limits on ultra-high-energy gamma-ray fluxes over four orders in magnitude in energy. These limits are not only of considerable astrophysical interest, but they also allow us to constrain beyond-standard-physics scenarios. For instance, dark matter particles could be superheavy, provided their lifetime is much longer than the age of the universe. Constraints on specific extensions of the Standard Model of particle physics that meet the lifetime requirement for a superheavy particle will be presented. They include limits on instanton strength as well as on mixing angle between active and sterile neutrinos.

§1 *Searches for ultra-high energy gamma-rays from dark-matter particles.* Compelling evidence for the observation of the decay of super-heavy dark matter particles would be the detection of a flux of gamma-rays with energies in excess of 10^8 GeV, in particular from regions of higher dark-matter density such as the center of our Galaxy. The identification of gamma-ray primaries relies on distinct salient features between the extensive air showers initiated by gamma-rays and those by the overwhelming background of nuclei: a lower number of secondary muons and deeper X_{\max} values. Both the ground signal and X_{\max} can be measured at the Pierre Auger Observatory [1] where a hybrid detection technique is employed for the observation of extensive air showers by combining fluorescence detectors with ground arrays of particle detectors. The combination of the various instruments allows ultra-high-energy gamma-rays to be detected in the energy range above $10^{7.7}$ GeV with a directional exposure obtained through the time and area integration of the detection efficiency ϵ_γ and selection efficiency κ_γ projected onto the direction perpendicular to the arrival direction,

$$\mathcal{E}_\gamma(E, \delta, \alpha) = \int d\mathbf{x} \int dt \cos\theta \epsilon_\gamma(E, \theta, \mathbf{x}, t) \kappa_\gamma(E, \theta). \quad (1)$$

In total, four different analyses, differing in the detector used, have been developed to cover the wide energy range probed at the Observatory [2, 3, 4, 5]. In particular, two of these analyses benefit from a direct estimate of the depth of shower maximum by the fluorescence detector as one of the discriminating variables. The use of the fluorescence-detector datasets introduces for these analyses an explicit dependence in time for ϵ_γ due to the limited

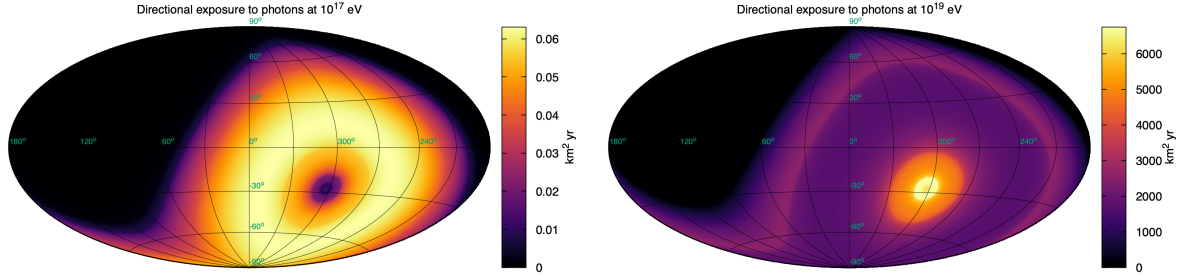


Figure 1: Directional exposure of the Pierre Auger Observatory in Galactic coordinates to ultra-high energy gamma-rays at 10^8 GeV (left) and 10^{10} GeV (right). From [6].

duty cycle on moonless nights that propagates into a small dependence in right ascension α for \mathcal{E}_γ . In addition to the detection efficiency, the κ_γ factor accounts for the dependencies of the selection process aimed at separating hadronic-induced showers from gamma-ray-induced ones. For illustration, we show in Fig. 1 an example of directional exposure to photons at 10^8 GeV (left panel) and at 10^{10} GeV (right panel). The former is built on the 1.14 km^2 array with a separation of detectors of 433 m optimized to study the range of energies around 10^8 GeV, while the latter is the $3,000 \text{ km}^2$ one, optimized for higher energies. This explains the large increase of exposure observed at high energies. Overall, no gamma-ray could be firmly identified up to now. The non-observation of candidates (beyond the expected background) allowed the derivation of upper bounds that can constrain various models very effectively, as discussed below.

Due to their attenuation over intergalactic distances, only ultra-high energy gamma-rays emitted in the Milky Way can survive on their way to Earth. The emission rate per unit volume and unit energy q_γ from decaying dark-matter particles is shaped by the energy density of dark matter ρ_{DM} ,

$$q_\gamma(E, \mathbf{x}_\odot + s\mathbf{u}) = \frac{1}{M_X \tau_X} \frac{dN_\gamma}{dE} \rho_{\text{DM}}(\mathbf{x}_\odot + s\mathbf{u}), \quad (2)$$

where M_X is the mass of the dark-matter particle, τ_X its lifetime, dN_γ/dE is the energy spectrum of the gamma-ray decay byproducts, \mathbf{x}_\odot is the position of the Solar system in the Galaxy, and \mathbf{u} is a unit vector on the sphere. The energy density is normalized to $\rho_\odot = 0.45 \text{ GeV cm}^{-3}$ [7]. The flux (per steradian) of ultra-high energy gamma-rays produced by the decay of dark-matter particles, $J_{\text{DM},\gamma}(E, \mathbf{u})$, is then obtained by integrating the position-dependent emission rate q_γ along the path of the photons in the direction \mathbf{u} ,

$$J_\gamma(E, \mathbf{u}) = \frac{1}{4\pi} \int_0^\infty ds q_\gamma(E, \mathbf{x}_\odot + s\mathbf{u}), \quad (3)$$

where the 4π normalization factor accounts for the isotropy of the decay processes. Finally, the expected number of events above a threshold energy follows from

$$n_\gamma(E) = \int d\mathbf{u} \int_{>E} dE' \mathcal{E}_\gamma(E', n) J_\gamma(E', \mathbf{u}). \quad (4)$$

Assuming that the relic abundance of dark matter is saturated by super-heavy particles, constraints can be inferred in the plane (τ_X, M_X) by requiring the number of gamma-rays expected from Eq. 4 to be less than the upper limits on the number of observed events accounting for the expected background. For generic two-body decay channels, the constraints generally lead to lifetime much longer than the age of the universe for $M_X > 10^9$ GeV.

§2 Lifetime constraints in the perturbative domain. To comply with the lifetime constraints, some models postulate the existence of super-weak couplings between the dark and standard-model sectors. The lifetime τ_X of the particles is then governed by the strength of the couplings $g_{X\Theta}$ (or reduced couplings $\alpha_{X\Theta} = g_{X\Theta}^2/(4\pi)$) and by the mass dimension n of the operator Θ standing for the standard model fields in the effective interaction [8]. Even without knowing the theory behind the decay of the dark-matter particle, generic constraints on $\alpha_{X\Theta}$ and n can be derived [9]. The effective interaction term that couples the field X associated with the heavy particle to the standard-model fields is taken as

$$\mathcal{L}_{\text{int}} = \frac{g_{X\Theta}}{\Lambda^{n-4}} X \Theta, \quad (5)$$

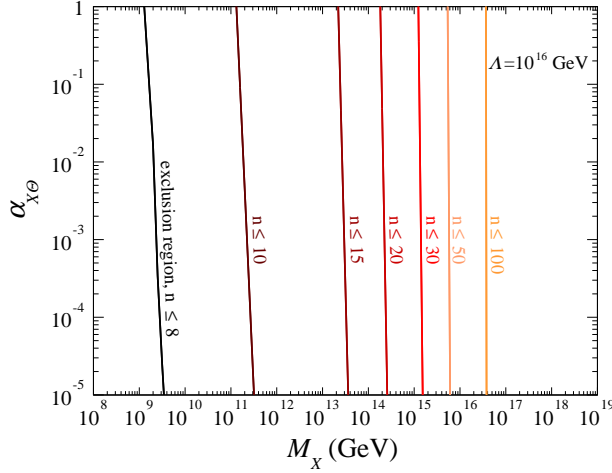


Figure 2: Exclusion regions in the plane $(\alpha_{X\Theta}, M_X)$ for several values of mass dimension n of operators responsible for the perturbative decay of the super-heavy particle, and for an energy scale of new physics $\Lambda = 10^{16}$ GeV. From [9].

where Λ is an energy parameter typical of the scale of the new interaction. In the absence of further details about the operator Θ , the matrix element describing the decay transition is considered flat in all kinematic variables so that it behaves as $|\mathcal{M}|^2 \sim 4\pi\alpha_{X\Theta}/\Lambda^{2n-4}$. On the basis of dimensional arguments, the lifetime of the particle X is then given as

$$\tau_{X\Theta} = \frac{V_n}{4\pi M_X \alpha_{X\Theta}} \left(\frac{\Lambda}{M_X} \right)^{2n-8}, \quad (6)$$

where V_n is a phase space factor. As a proxy for this factor, we use the expression derived for $n-1$ particles in the final state [10],

$$V_n = \left(\frac{2}{\pi} \right)^{n-1} \Gamma(n-1)\Gamma(n-2), \quad (7)$$

with $\Gamma(x)$ the Euler gamma function. It is apparent that the coupling constant $\alpha_{X\Theta}$ and the dimension n have to take specific values for super-heavy particles to be stable enough. In practice, for a specific upper limit on $n_\gamma(E)$ at one energy threshold E , a lower limit of the $\tau_{X\Theta}$ parameter is derived for each value of mass M_X . The lower limit on $\tau_{X\Theta}$ is subsequently transformed into an upper limit on $\alpha_{X\Theta}$ by means of Eq. (6). By repeating the procedure for each upper limit on $n_\gamma(E)$, a set of curves is obtained, reflecting the sensitivity of a specific energy threshold to some range of mass. The union of the excluded regions finally provides the constraints in the plane $(\alpha_{X\Theta}, M_X)$. In this manner we obtain the contour lines shown in Fig. 2 for several values of n and for an emblematic choice of GUT Λ value. The scale chosen for $\alpha_{X\Theta}$ ranges from 1 down to 10^{-5} . It is observed that for the limits on photon fluxes to be satisfied, the mass of the super-heavy particle cannot exceed $\gtrsim 10^9$ GeV ($\gtrsim 10^{11}$ GeV) for operators of dimension equal to or larger than $n=8$ ($n=10$), while larger masses require an increase in n . To approach the large masses while keeping operators of dimension relatively low, “astronomically-small” coupling constants should be at work. The same conclusions hold for other choices of Λ . All in all, for perturbative processes to be responsible for the decay of super-heavy dark matter particles requires quite “unnatural” fine-tuning.

§3 *Constraints on instanton-induced decays.* Stability of super-heavy dark matter particles is consequently calling for a new quantum number to be conserved in the dark sector so as to protect the particles from decaying. Nevertheless, even stable particles in the perturbative domain will in general eventually decay due to non-perturbative effects (instantons) in non-abelian gauge theories. Instanton-induced decay can thus make observable a dark sector that would otherwise be totally hidden by the conservation of a quantum number [11]. Assuming quarks and leptons carry this quantum number and so contribute to anomaly relationships with contributions from the dark sector, they will be secondary products in the decays of dark matter together with the lightest hidden fermion. The lifetime of the decaying particle is mainly driven by the instanton suppression factor that leads to [12]

$$\tau_X \simeq M_X^{-1} \exp(4\pi/\alpha_X), \quad (8)$$

with α_X the reduced coupling constant of the hidden gauge interaction.

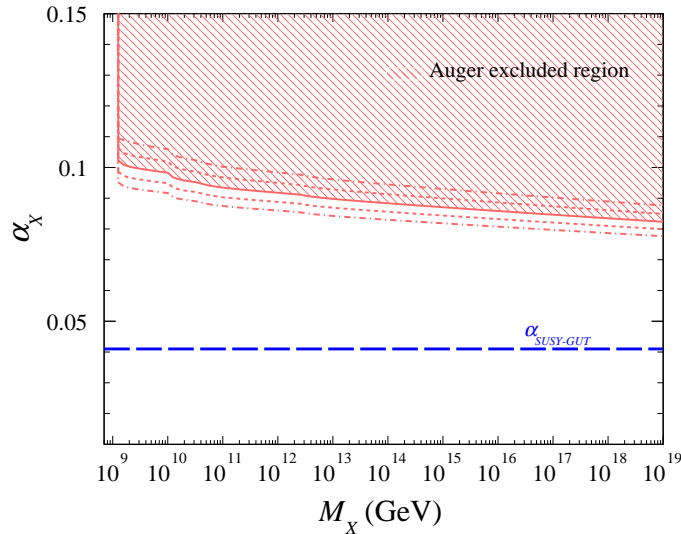


Figure 3: Upper limits at 95% C.L. on the coupling constant α_X of a hidden gauge interaction as a function of the mass M_X of a dark matter particle X (assumed to compose 100% of the observed dark matter abundance) decaying into a dozen of $q\bar{q}$ pairs. From [13].

Quite independently of the hidden gauge interaction, the exact content in instanton-induced decays of quarks and leptons, which will eventually produce hadrons decaying into photons and neutrinos, obeys selection rules that involve very large multiplicities. Assuming ten pairs of quarks and leptons in the final state, the energy spectrum $dN_\gamma(E, M_X)/dE$ then follows from fragmentation effects [14, 15, 16, 17].

Eq. (8) provides us with a relationship connecting the lifetime τ_X to the coupling constant α_X . In the same way as in the perturbative case above, upper limits on α_X can be obtained. They are shown as the shaded red area in Fig. 3. The coupling should be less than ≈ 0.09 for a wide range of masses. Numerical factors in front of the exponential could however arise in Eq. (8) depending on the underlying model for the hidden gauge sector. Explicit constructions of the dark sector are, however, well beyond the scope of this contribution. Although the limits presented in Fig. 3 are hardly destabilized due to the exponential dependence in α_X^{-1} , we note that model-dependent numerical factors in front of the exponential such as $10^{\pm k}$ lead to a shift of $\pm 0.0013k$ in α_X limits. We show in dotted and dashed lines the bounds for $k = 2$ and $k = 4$, respectively. These factors are by far the dominant systematic uncertainties.

§4 *Constraints on dark matter coupled to sterile neutrinos.* A superheavy particle that is metastable can also result from the coupling between a pseudo-scalar particle with sterile neutrinos embedded in an extended-seesaw framework [18]. In this beyond-standard-model extension, the dark-matter particle X interacts only with sub-eV and superheavy (10^{12-14} GeV) sterile neutrinos, of masses m_N and M_N respectively, via Yukawa couplings y_m and y_M . In the mass-eigenstate basis, neutrinos ν_1 and ν_2 are then quasi-sterile or quasi-active respectively, depending on the mixture of active and sterile neutrinos governed by a small mixing angle $\theta_m \simeq \sqrt{2}y_mv/m_\nu$, with v the electroweak scale (mass dimension) and m_ν the mass of the known neutrinos. To leading order in y_m , quasi-active neutrinos are produced from quasi-sterile ones subsequent to the decay of X . Consequently, the coupling y_m controls the dominant decay channels and allows for trading a factor $(M_X/M_P)^2$ (with M_P the Planck mass) for a $(m_\nu\theta_m/v)^2$ one in the decay width of X . This trading enables the reduction of the width by a factor $\sim 10^{-25}\theta_m^2$ for a benchmark value $M_X = 10^9$ GeV, leading to the required lifetimes well beyond the age of the universe.

To leading order in θ_m , the total width Γ^X is dominated by three-body channels stemming from the interaction between active/sterile neutrinos and the Higgs isodoublet with Yukawa coupling $y_m \simeq \sqrt{2}\theta_m m_2/v$. The channel

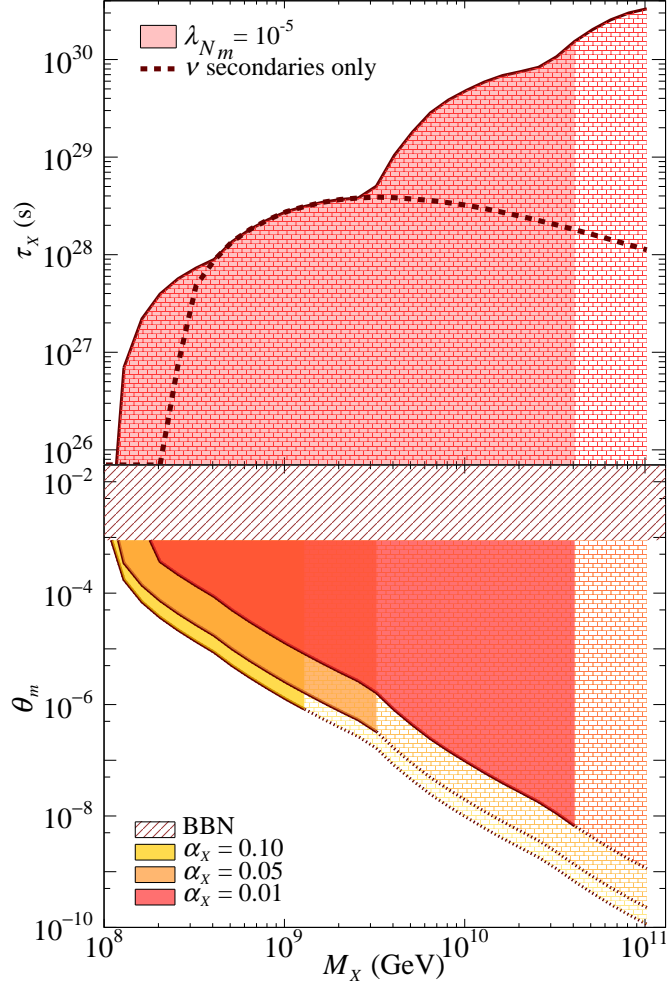
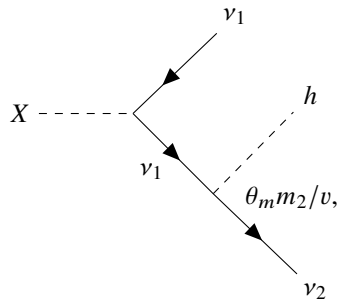


Figure 4: *Top*: Constraints on τ_X as a function of M_X for a value of the couplings of sterile neutrinos with the inflationary sector $\lambda_{N_m} = 10^{-5}$. The dotted line illustrates the constraints stemming from neutrino secondaries alone. *Bottom*: Constraints on θ_m as a function of M_X for three different values of the coupling constant α_X , still for $\lambda_{N_m} = 10^{-5}$. The hatched-red region $\theta_m \geq 9 \times 10^{-4}$ is excluded from the constraint on ΔN_{eff} (see text). From [6].

$X \rightarrow h\nu_1\nu_2$, diagrammatically represented as



(9)

gives the most important contribution to the width [18]:

$$\Gamma_{h\nu_1\nu_2}^X = \frac{\alpha_X^2 \theta_m^2}{192\pi^3} \left(\frac{M_X}{M_{\text{P}}}\right)^2 \left(\frac{m_2}{v}\right)^2 M_X. \quad (10)$$

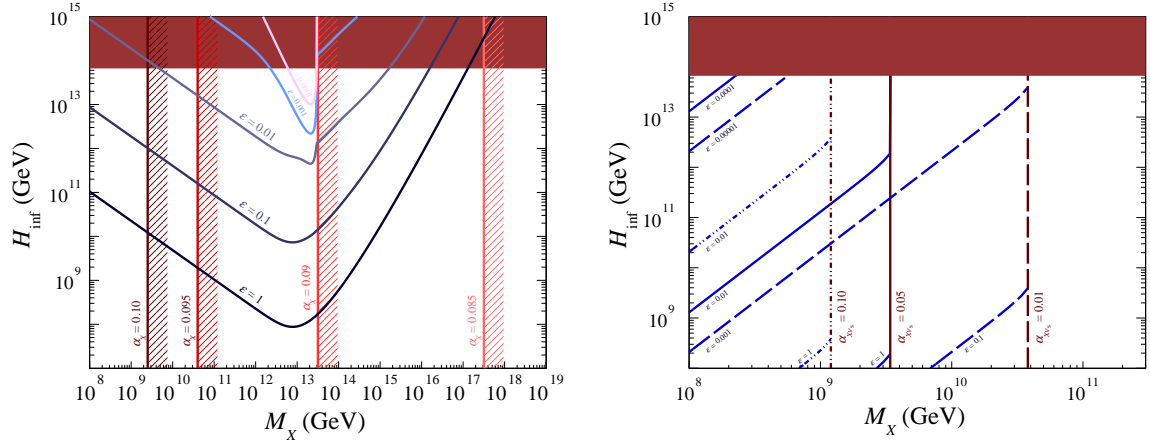


Figure 5: Left: Constraints in the (H_{inf}, M_X) plane, where viable values are delineated by the blue lines for different values of reheating efficiency ϵ . Additional constraints from the non-observation of instanton-induced decay of super-heavy particles allow for excluding the mass ranges in the red-shaded regions, for the specified value of the dark-sector gauge coupling. From [13]. Right: Same, adding the possibility of a radiative production of dark matter in the inflaton decay.

As announced, a factor $(M_X/M_{\text{P}})^2$ expected from dimensional arguments is indeed traded for a factor $(m_2/v)^2$. Constraints in the planes (τ_X, M_X) and (θ_m, M_X) can be derived from the non-observation of ultra-high energy gamma-rays (and neutrinos) at the Observatory. First, 90% C.L. lower limits on the lifetime τ_X are obtained as previously by setting, for a specific value of M_X , $n_\gamma(E)$ or $n_\nu(E)$ to the 90% C.L. upper-limit numbers corresponding to the number of background-event candidates in the absence of signal. Subsequently, a scan in M_X is carried out. It leads to a curve in the plane (τ_X, M_X) that pertains to the energy threshold E considered. By repeating the procedure for several thresholds, a set of curves is obtained, reflecting the sensitivity of a specific energy threshold to some range of mass M_X . The union of the excluded regions finally provides the constraints in the (τ_X, M_X) plane. Results are shown in Fig. 4 (top panel); lifetimes within the cross-hatched region are excluded. The region in full red pertains to a particular value of a Yukawa coupling $\lambda_{N_m} = 10^{-5}$, the meaning of which will be explained below. To illustrate the contribution from each secondary at our disposal, we show as the dotted the contribution to the constraints stemming from neutrinos alone; an analysis of the IceCube exposure dedicated to the benchmark-scenario decay channels would likely provide better sensitivity for exploring masses $M_X \lesssim 10^{8.5}$ GeV. The lower limit on τ_X is then transformed into an upper limit on θ_m using the expressions of the total width of the particle X . Results are shown in the bottom panel for separate values of α_X : color-coded regions pertain to $\lambda_{N_m} = 10^{-5}$ while their extension (in cross-hatched) would require smaller values of λ_{N_m} . Systematic uncertainties on θ_m constraints amount overall to $\simeq \pm 15\%$; they are dominated by those on the neutrino exposure [19]. The restricted ranges of M_X for different α_X values come from the requirements not to overclose the universe with dark matter, while the exclusion hatched band comes from not altering the expansion history of the universe with the presence of ultra-light species such as sterile neutrinos N_m . We now briefly explain how these constraints are obtained.

§5 Cosmological constraints. Gravitational interaction alone may have been sufficient to produce the right amount of super-heavy dark matter particles at the end of the inflation era for a wide range of high masses, up to M_{GUT} , accounting for the production by annihilation of standard model particles (SM) [20] or of inflaton particles (ϕ hereafter) [21] through the exchange of a graviton. In this scenario, the relic abundance of super-heavy dark matter particles can be estimated from the quite involved reheating dynamics [22, 23]. The time evolution of the X -particle density n_X reads as

$$\frac{dn_X(t)}{dt} + 3H(t)n_X(t) \simeq \sum_i \bar{n}_i^2(t)\gamma_i, \quad (11)$$

where the sum in the right hand side stands for the contributions from the standard model [20] and inflationary [21] sectors to produce fermions. Introducing the dimensionless abundance $Y_X = n_X a^3 / T_{\text{rh}}^3$ to absorb the expansion of the universe, with T_{rh} the reheating temperature, and using $aH(a)dt = da$ from the definition of the Hubble

parameter (with a the scale factor), Eq. 11 becomes

$$\frac{dY_X(a)}{da} \simeq \frac{a^2}{T_{\text{rh}}^3 H(a)} \sum_i \bar{n}_i^2(a) \gamma_i, \quad (12)$$

which, using the dynamics of the expansion rate during reheating, yields the present-day dimensionless abundance $Y_{X,0}$ assuming $Y_{X,\text{inf}} = 0$. The present-day relic abundance, Ω_{CDM} , can then be related to M_X , H_{inf} , and $\epsilon = T_{\text{rh}}/(0.25\sqrt{M_{\text{P}}H_{\text{inf}}})$ through [20] $\Omega_{\text{CDM}}h^2 = 9.2 \cdot 10^{24} \epsilon^4 M_X Y_{X,0}/M_{\text{P}}$. As a result, one interesting viable possibility in the (H_{inf}, M_X) parameter space is that X particles with masses as large as the GUT energy scale could be sufficiently abundant to match the dark matter relic density, provided that the inflationary energy scale is high ($H_{\text{inf}} \sim 10^{13}$ GeV) and the reheating efficiency is high (so that reheating is quasi-instantaneous). This rules out values of the dark-sector gauge coupling greater than $\simeq 0.085$, as observed in the left panel of Fig. 5. The mass values could however be smaller if the reheating temperature is not that high. In general, for high efficiencies ϵ (corresponding to short duration of the reheating era), the $\text{SM} + \text{SM} \rightarrow X + X$ reaction allows for a wide range of M_X values. For efficiencies below $\simeq 0.01$, the $\phi + \phi \rightarrow X + X$ reaction allows for solutions in a narrower range of the (H_{inf}, M_X) plane close to $M_X = 10^{13}$ GeV, with in particular $M_X \leq M_\phi$ as a result of the kinematic suppression in the corresponding rate γ_i [21].

Similar constraints can be drawn for the model invoking couplings of the X particle with sterile neutrinos. In addition to its couplings to the dark-matter sector and to the standard-model one through the Higgs isodoublet, the sterile neutrino N_m is also coupled to an inflationary sector in the benchmark [18]. This coupling, governed by a unique Yukawa parameter λ_{N_m} for every ν_1 neutrinos, yields to a ‘‘radiative’’ production of X via a diagram similar to that depicted in Eq. 9 (substituting X by the inflaton Φ in the initial state, and h and ν_2 by X and ν_1 in the final states). Such a mechanism leads to a direct production of dark matter during the reheating period that can be sufficient, in general, to match the right amount of dark matter observed today [24]. In the benchmark [18], values for λ_{N_m} are then required to range preferentially around 10^{-5} . To infer the dark matter density n_X produced mainly during the reheating epoch, we also consider the minimal setup of gravitational production of X particles through the annihilation of standard-model (inflaton) particles as in [20] (as in [21]). In these conditions, X particles can be produced as long as the collision rate of particles is larger than the expansion rate H and/or as long as the inflaton field oscillates. By contrast, n_X is prohibitively low to allow any thermal equilibrium for dark matter. The collision term in the Boltzmann equation is then approximated as a source term only. Overall, the Boltzmann equation reads as

$$\frac{dn_X(t)}{dt} + 3H(t)n_X(t) = \sum_i \bar{n}_i^2(t) \gamma_i + \bar{n}_\phi(t) \Gamma_{X\nu_1\nu_1}. \quad (13)$$

As a result, viable couples of values for (H_{inf}, M_X) scale as $H_{\text{inf}} \propto M_X^2$ up to a maximum value for M_X , which depend on ϵ and α_X – see right panel of Fig. 5. This scaling is a consequence of the domination of the radiative-production process over the gravitational one as long as the allowed values of H_{inf} are too small for a given M_X value to generate significant particle production by gravitational interactions. For larger masses, the contribution from gravitational interactions added to the radiative production of X leads to an overproduction of dark matter that overcloses the universe, and there is thus no longer solution. This explains why the color-coded regions extend up to some maximum values of M_X in Fig. 4, for a benchmark value of $\lambda_{N_m} = 10^{-5}$. To the right of the regions shown in cross-hatched, λ_{N_m} would need to be smaller.

§6 Conclusions. We have shown that the data of the Pierre Auger Observatory provide stringent constraints on decaying super-heavy particles that would constitute dark matter. These constraints allow us to put a limit on instanton strength or on the angle θ_m mixing sub-eV sterile and active neutrinos in the context of an extension to the SM that couples the sterile neutrinos to a superheavy DM candidate. Other physics providing mechanisms to stabilize super-heavy particles can be explored, such as supersymmetry broken at high scale with a tiny R -parity violation. This will be the subject of a future study.

References

- [1] Aab A et al. (Pierre Auger) 2015 Nucl. Instrum. Meth. A **798** 172–213 (*Preprint* 1502.01323)
- [2] Abdul Halim A et al. (Pierre Auger) 2023 PoS ICRC2023 238
- [3] Abreu P et al. (Pierre Auger) 2022 Astrophys. J. **933** 125 (*Preprint* 2205.14864)
- [4] Abdul Halim A et al. (Pierre Auger) 2024 (*Preprint* 2406.07439)
- [5] Abreu P et al. (Pierre Auger) 2023 JCAP **05** 021 (*Preprint* 2209.05926)
- [6] Abdul Halim A et al. (Pierre Auger) 2024 Phys. Rev. D **109** L081101 (*Preprint* 2311.14541)
- [7] Jiao Y, Hammer F, Wang H, Wang J, Amram P, Chemin L and Yang Y 2023 Astron. Astrophys. **678** A208 (*Preprint* 2309.00048)
- [8] de Vega H J and Sanchez N G 2003 Phys. Rev. D **67** 125019
- [9] Abreu P et al. (Pierre Auger) 2023 Phys. Rev. D **107** 042002 (*Preprint* 2208.02353)
- [10] Kleiss R, Stirling W J and Ellis S D 1986 Comput. Phys. Commun. **40** 359
- [11] Kuzmin V A and Rubakov V A 1998 Phys. Atom. Nucl. **61** 1028 (*Preprint* astro-ph/9709187)
- [12] 't Hooft G 1976 Phys. Rev. Lett. **37** 8–11
- [13] Abreu P et al. (Pierre Auger) 2023 Phys. Rev. Lett. **130** 061001 (*Preprint* 2203.08854)
- [14] Aloisio R, Berezhinsky V and Kachelriess M 2004 Phys. Rev. D **69** 094023 (*Preprint* hep-ph/0307279)
- [15] Sarkar S and Toldra R 2002 Nucl. Phys. B **621** 495–520 (*Preprint* hep-ph/0108098)
- [16] Barbot C and Drees M 2003 Astropart. Phys. **20** 5–44 (*Preprint* hep-ph/0211406)
- [17] Bauer C W, Rodd N L and Webber B R 2021 JHEP **06** 121 (*Preprint* 2007.15001)
- [18] Dudas E, Heurtier L, Mambrini Y, Olive K A and Pierre M 2020 Phys. Rev. D **101** 115029 (*Preprint* 2003.02846)
- [19] Aab A et al. (Pierre Auger) 2019 JCAP **10** 022 (*Preprint* 1906.07422)
- [20] Garny M, Sandora M and Sloth M S 2016 Phys. Rev. Lett. **116** 101302 (*Preprint* 1511.03278)
- [21] Mambrini Y and Olive K A 2021 Phys. Rev. D **103** 115009 (*Preprint* 2102.06214)
- [22] Chung D J H, Kolb E W and Riotto A 1999 Phys. Rev. D **60** 063504 (*Preprint* hep-ph/9809453)
- [23] Giudice G F, Kolb E W and Riotto A 2001 Phys. Rev. D **64** 023508 (*Preprint* hep-ph/0005123)
- [24] Kaneta K, Mambrini Y and Olive K A 2019 Phys. Rev. D **99** 063508 (*Preprint* 1901.04449)